TECHNICAL PAPER

Proton beam writing: a platform technology for nanowire production

J. A. van Kan · F. Zhang · S. Y. Chiam · T. Osipowicz · A. A. Bettiol · F. Watt

Abstract P-beam writing (proton beam writing) is a unique direct write 3D nano-lithographic technique which has been developed at the Centre for Ion Beam Applications (CIBA), in the Physics Department of the National University of Singapore. This technique employs a focused MeV proton beam which is scanned in a predetermined pattern over a resist (e.g. PMMA, SU-8 or HSQ), which is subsequently chemically developed. In e-beam writing as well as p-beam writing the energy loss of the primary beam is dominated by energy transfer to substrate electrons. Unlike the high energy secondary electrons generated during e-beam writing the secondary electrons induced by the primary proton beam have low energies (typically less than 100 eV) and therefore a limited range, resulting in minimal proximity effects. The low proximity effects exhibited by p-beam writing coupled with the straight trajectory and high penetration of the proton beam enables the production of high aspect ratio, high density 3D micro- and nano-structures with well defined smooth side walls to be directly written into resist materials. These structures can be used as templates to electroplate metallic nanowires.

J. A. van Kan (✉) · A. A. Bettiol
Engineering Science Programme,
Centre for Ion Beam Applications (CIBA),
Department of Physics, National University of Singapore,
2 Science Drive 3, Singapore 117542, Singapore
e-mail: phyjavk@nus.edu.sg

F. Zhang · S. Y. Chiam · T. Osipowicz · F. Watt
Centre for Ion Beam Applications (CIBA),
Department of Physics, National University of Singapore,
2 Science Drive 3, Singapore 117542, Singapore

1 Introduction

Nanowires are a potential building block for nano-electronics devices (Thelander et al. 2006). Application can be found in areas like nanowire transistors (Chen et al. 2004) and magnetoelectrical devices. In the latter case magnetic materials with periodically modulated layers at the nanometer scale have been explored (Kruglyak et al. 2005; Pramanik et al. 2006). The discovery of giant magnetoresistance (GMR) effect in Fe/Cr multilayers (Baibich et al. 1988) has attracted extensive interest. Two type of structures with GMR properties i.e. spinvalves and multilayers are currently used for magnetic sensor applications (Liu et al. 2003). One challenge in achieving nano-electronic devices is the integration of nano-wires to form contacts (Qin et al. 2005; Martin and Baker 2005).

Essentially no proximity effects have been observed in p-beam writing experiments (van Kan et al. 2003a) so far. We have recently introduced hydrogen silsesquioxane (HSQ), a non C based resist, as a new resist for p-beam writing allowing the fabrication of 22 nm details standing at a height of 850 nm (van Kan et al. 2006). The results obtained with p-beam writing using the HSQ resist, show that HSQ behaves as a high resolution negative resist under proton beam exposure. HSQ, (produced by Dow Corning) was introduced as a high resolution negative tone e-beam resist by Namatsu et al. (1998). Our current research aims at the integration of 3D nano-rod structures through high aspect ratio nano-fabrication using p-beam writing. The successful production of such structures via electroplating and selective etching will open up the possibility to integrate nanowires into functional devices. Here we present initial studies on process parameters of PMMA resist in combination with p-beam writing as a plating base (van Kan et al. 2001; Ansari et al. 2004) for nanowire

production. The PMMA written templates have been used successfully in combination with Ni and Au electroplating to make high aspect ratio Ni and Au nanowires.

2 Experimental procedures

P-beam writing employs a focused MeV proton beam scanned in a pre-determined pattern over a suitable resist. The work discussed here has been carried out at the CIBA using a 3.5 MV HVEE Singletron™ accelerator coupled to a dedicated p-beam writing set-up. In this system protons are focused down with a high excitation triplet of compact magnetic quadrupole lenses (OM52-Oxford Microbeams) (Breese et al. 1999) which demagnifies a beam defining object slit into the proton beam writing exposure-station (Watt et al. 2003; van Kan et al. 2003b). This is a unique system, since it is dedicated to p-beam writing on micron and nano scales. With the introduction of HSQ (van Kan et al. 2006) there are now three known high resolution resists for p-beam writing. HSQ, PMMA and SU-8 have all shown sub 100 nm capabilities in combination with p-beam writing (van Kan et al. 2007). To fabricate holes which can function as templates to electroplate metallic nanowires PMMA is the choice since it is the only high resolution positive resist for p-beam writing. Earlier results have shown that accurate high aspect ratio nanostructures can be produced in PMMA and SU-8 with a typical RMS sidewall roughness of less than 3 nm (van Kan et al. 2003a). In many applications it is important to have perfect side wall verticality as well as smooth sidewalls. SRIM (Biersack and Haggmark 1980) calculations show that a parallel incoming proton beam will spread less than 8.0 nm (90% of the beam) after penetrating 2 µm in PMMA. Secondary electron excitation calculations (Waligorski et al. 1986) show that 90% of the energy will be deposited within 3.0 nm of the proton track using a 2 MeV proton beam in 2-µm thick PMMA. Taking these two facts into consideration we can expect a sidewall verticality of about 89.7° if we write structures in a 2-µm thick resist layer. Similarly we can expect a side wall verticality of 89.4° if we write structures in a 10 µm thick resist layer (van Kan et al. 2003a, 2000).

Electroplating requires the sample to have an adequate metallic seed layer. Since protons are not affected by the underlying substrates (van Kan et al. 2004a) and no proximity effects have been observed (van Kan et al. 2003a, 2006), we can choose any metallic layer as substrate. Here two different samples were prepared. In both cases Si wafers were pre-coated with a thin Au layer which acts as a seed layer for electroplating and a thin Cr layer acting as a glue layer. Before spincoating, the two wafers were dry baked at 180°C for 20 min followed by air cooling for

3 min. The first wafer was spincoated using A4, 950 K molecular weight PMMA resist in anisole from Mirco-Chem using two coats at 1,000 RPM. After the first coat, a baking step of 3 min at 180°C was applied. After the second coat, an 8-min bake at 180°C was applied. During the baking a gentle N_2 flow was applied to guarantee the wafer is kept dry, this is to ensure good adhesion of the resist to the substrate. Following this procedure an 850 nm thick PMMA layer was obtained. The second wafer was coated with A11, 950 K molecular weight PMMA resist in anisole from MircoChem. Here three coats were applied after every coat the wafer was baked at 180 C for 8 min in a N_2 atmosphere. This procedure resulted in a 10 µm thick PMMA layer.

In the p-beam writing experiments the dose was varied from 80 nC/mm² up to 200 nC/mm² using 2 MeV protons. All the samples exposed with the proton beam were developed in iso-propyl alcohol (IPA) and water (7:3). The development time was varied from 2 to 10 min depending on the thickness of the resist and the number of protons used to expose holes in the PMMA. We have observed previously that it is better to use this less viscous developer compared to the conventional GG developer (Springham et al. 1997) for the production of high aspect ratio confined nanostructures (van Kan et al. 2003a, 2004b).

Two types of electroplating are presented; firstly Au plating was performed in a beaker set-up using Microfab Au-100 from Enthone at 60°C, here typical plating current densities are 0.25 mA/cm², this corresponds to a plating rate of 200 nm /min. Secondly Ni electroplating was performed in a Technotrans AG, RD.50 plating system, using a Ni Sulphamate solution at 50°C. Typical current densities used are 1–2 mA/cm², this corresponds to a plating rate of 25 nm/min.

In a first test sub micrometer holes were exposed in a 10 µm thick PMMA layer. To obtain the desired sized holes a 2 MeV proton beam was focused to sub micron dimensions and used to irradiate a row of single dots separated by 10 µm. Next the sample was developed for 10 min followed by a DI water rinse. In this experiment Au pillars were electroplated up to a thickness of 6.1 µm. After electroplating the resist was removed in toluene at 40°C for 1 h. As can be seen in Fig. 1a, b smooth parallel Au pillars of 700 × 880 nm² are obtained.

In order to get a more even energy deposition across the surface of the holes in PMMA in a next experiment the proton beam was focused down to 137 × 205 nm² and scanned over the holes in a pattern of two concentric circles with a radius of 100 and 250 nm, aiming at 1 µm holes, see Fig. 2a. Here a matrix of 7 × 7 holes are written, spaced 50 µm apart, in the 10 µm thick layer of PMMA. Every hole was exposed with 450 k protons. After proton beam exposure the sample was developed for 10 min followed by
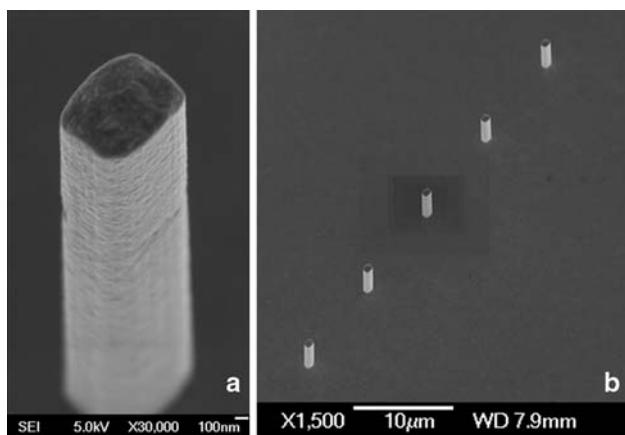
Fig. 1 SEM micrograph of 6.1 μm high pillars plated in Au. Here a 10 μm thick PMMA film was exposed with a focused 2 MeV proton beam following the "single dot" strategy

a rinse in DI water. The plating was aimed at half the height of the PMMA layer, resulting in pillars with a height of 5 μm. After plating the resist was removed in toluene at 40°C for 1 h. In Fig. 2b one of the plated Ni pillars is shown. As is clear from Fig. 2c not all the pillars remained standing. Careful electron microscopy study of the interface between the plated pillar which was detached and the substrate suggests there might be a fragmented thin film of undeveloped resist left, either due to insufficient
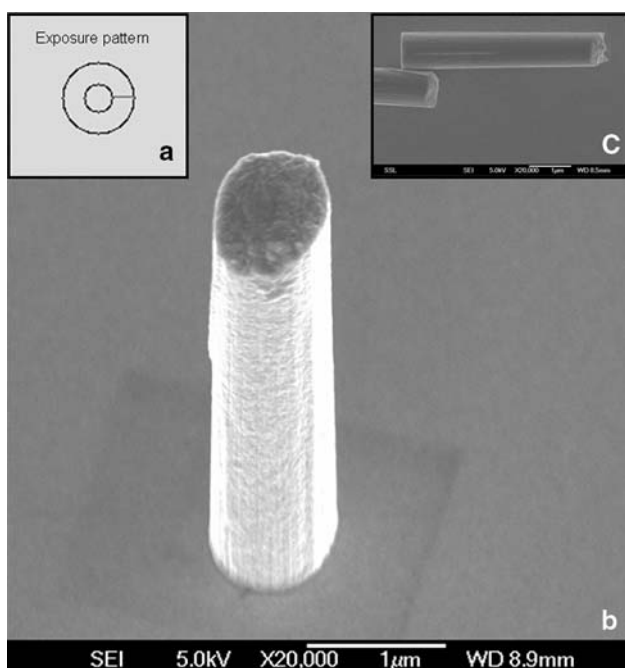
development time and or due to a low number of protons. From the fallen pillar we can measure the spread of the proton beam in the original resist from a depth of 5 μm down to 10 μm to be 0.6° from the parallel beam path, see Fig. 2c. This closely matches the spread calculated using SRIM (Biersack and Haggmark 1980; van Kan et al. 2000).

From here on, we will discuss pillars made using the "single dot" irradiation strategy, which is expected to result in the smallest diameter pillars. The holes were written in a matrix of 40×40 with a spacing of 1 μm. With the beam focused to 137×205 nm^2 an array of holes was written in the 10 μm thick PMMA film. Here three different numbers of protons were used to expose the individual pillars, i.e. 50, 75 and 150 k protons per pillar. The sample was developed for 10 min and the PMMA was removed as before. In the case of the low dose exposure only 5 out of the 1,600 pillars survived the fabrication
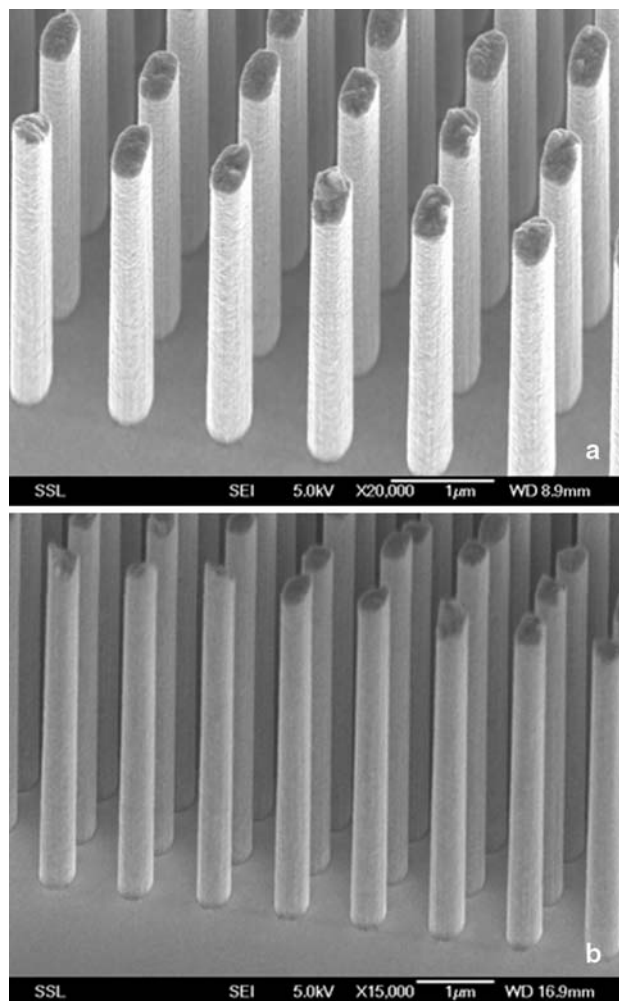

Fig. 2 SEM micrograph of 5 μm high Ni pillars (**b**). Here a 10 μm thick PMMA film was exposed with a focused 2 MeV proton beam following a specific exposure pattern (**a**). From the detached Ni pillar (**c**) the spread of the proton beam is estimated to be 0.6°

Fig. 3 SEM micrograph of 5 μm high pillars plated in Ni. Here a 10 μm thick PMMA film was exposed with a focused 2 MeV proton beam following the "single dot" strategy

Fig. 4 Proton induced secondary electron map of a Ni resolution standard with extracted horizontal and a vertical line scans. The FWHM fitted beam size is 98×195 nm^2
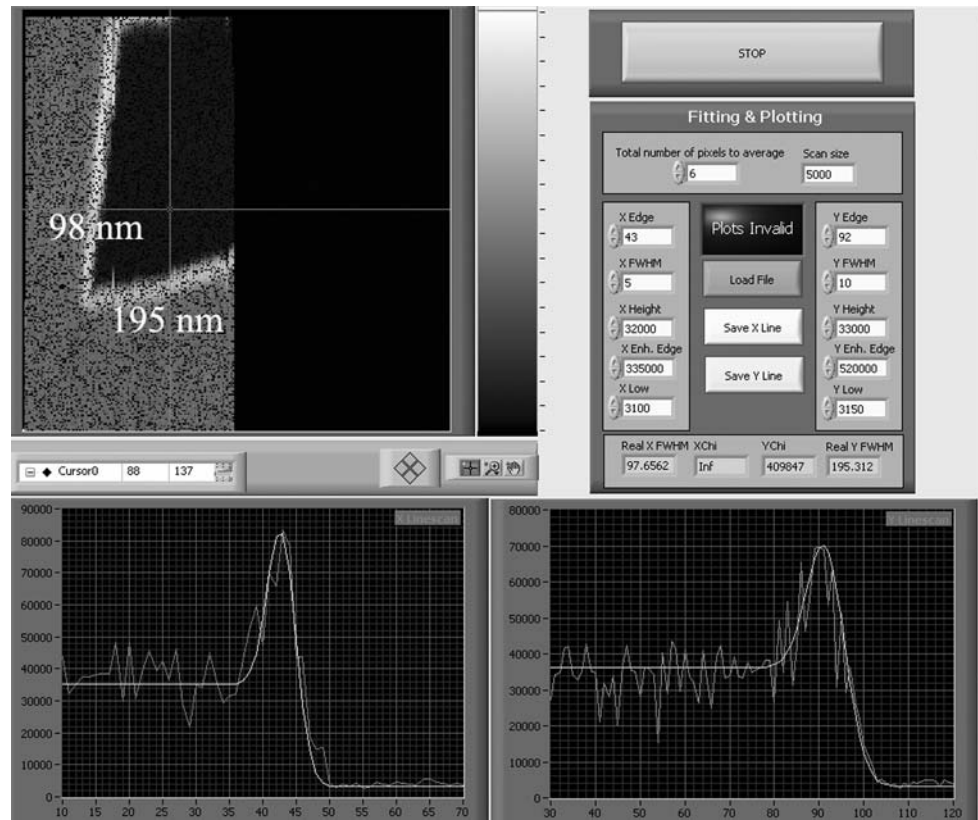
process. At 75 and 150 k protons per pillar practically all the pillars survived. In Fig. 3a and b two SEM micrographs are shown of the Ni pillars produced using the 75 k protons per pillar exposure, the size of the pillars is 310×570 nm^2 standing at a height of 5 μm.

To investigate the size discrepancy between the fitted beam size and the fabricated Ni pillars 12 sets of holes were exposed in the 850 nm thick PMMA layer on three different samples. In every sample four arrays of pillars were exposed using a beam focused down to 98×195 nm^2, see Fig. 4. Here the beam size was fitted following the procedure discussed by Udalagama et al. (2007). Every array of pillars consists out of a matrix of 40×40 pillars spaced 1 μm apart. The four arrays were exposed with 33, 44, 55 and 66 k protons per pillar. The three different samples were developed for 2, 4 and 10 min. After Ni electroplating the remaining PMMA was removed as described before, the sizes of the 12 different sets of Ni pillars was measured through SEM analysis, a summary of the results is shown in Fig. 5. In the case of the lowest dose and a 2 min development about 80% of the pillars survived the fabrication procedure. Doubling the development time, more than 99% of the pillars survived the fabrication steps here the pillars are not always parallel indicating too short development time and or a too low dose.
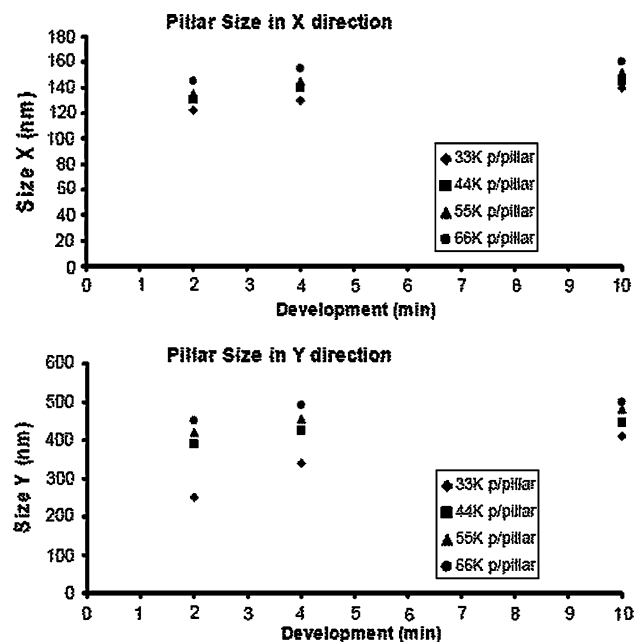

Fig. 5 Ni pillar sizes in *x* and *y* direction obtained as a function of development time for three different samples. Here an 850 nm thick PMMA layer was exposed with a focused 2 MeV proton beam following the "single dot" strategy with the proton beam focused down to 98×195 nm^2
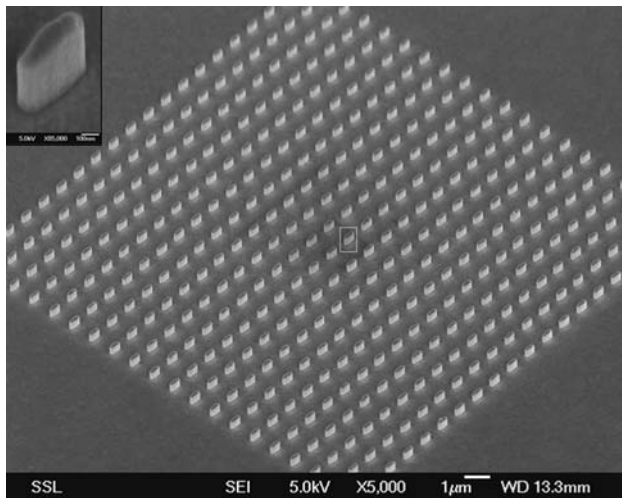
Fig. 6 SEM micrograph of 400 nm high Ni pillars. Here an 850 nm thick PMMA film was exposed with a focused 2 MeV proton beam following the "single dot" strategy

In Fig. 6 the Ni pillars produced using the 4 min development time and 55 k protons per pillar are shown. Here the Ni is plated up to a height of 400 nm. As is clear all the pillars are of high quality and as shown on the inset have smooth and parallel side walls. These pillars have a size of 145×455 nm^2.

3 Discussion

As is clear from Figs. 5 and 6 the proton beam has a longer tail in the y direction compared with the x direction, which is the low demagnification direction of the system. Therefore in order to get a small beam sizes in the y direction the beam defining object slits have to be set smaller compared with the x direction resulting in more scattered beam or "halo" (Watt et al. 2003). These effects are still under investigation. More research is planned to reduce the effects of beam scattering. The resolution standards used to determine the proton beam size have a side wall slope equivalent to about 14 nm, giving rise to inaccuracies in both the beam size and beam shape determination (van Kan et al. 2005; Zhang et al. 2007). It has been reported that there is an increase in brightness in particle accelerators near the paraxial region (Szymanski and Jamieson 1997). Control of these beam parameters will enable to the production of smaller metallic nanowires.

4 Conclusions

P-beam writing is capable of creating high aspect ratio polymer structures with sub 100 nm features, which can be used as molds to produce metallic nanowires. These initial studies show the fabrication of Au and Ni pillars with smooth sidewalls, details down to 120 nm level and aspect ratios up to 15. P-beam writing appears ideally suited to directly write PMMA templates with: nanometer sized dimensions, high aspect ratios and smooth and vertical sidewalls in a single-step process. In future experiments different development strategies will be tested to optimized the fabrication of metallic pillars at the 100 nm level and below. Therefore we expect p-beam writing to make a significant contribution towards the progress in nano-technology development.

References

Ansari K, van Kan JA, Bettiol AA, Watt F (2004) Fabrication of high aspect ratio 100 nm metallic stamps for nanoimprint lithography using proton beam writing. Appl Phys Lett 85:476–478

Baibich MN, Broto JM, Fert A, Nguyen VDF, Petroff F, Etienne P, Creuzt G, Friederich A, Chazelas J (1988) Giant magnetoresistance of (001)Fe/(001)Cr magnetic superlattices. Phys Rev Lett 61:2472–2475

Biersack J, Haggmark LG (1980) A Monte Carlo computer program for the transport of energetic ions in amorphous targets. Nucl Instr Meth 174:257–269

Breese MBH, Grime GW, Linford W, Harold M (1999) An extended magnetic quadrupole lens for a high-resolution nuclear microprobe. Nucl Instr Meth B158:48–52

Chen J, Klaumünzer S, Lux-Steiner MC, Könenkamp R (2004) Vertical nanowire transistors with low leakage current. Appl Phys Lett 85:1401–1403

Kruglyak VV, Hicken RJ, Kuchko AN, Gorobets VYu (2005) Spin waves in a periodically layered magnetic nanowire. J Appl Phys 98:014304-1–014304-4

Liu H-R, Ren T-L, Qu B-J, Liu L-T, Ku W-J, Li W (2003) The optimization of Ta buffer layer in magnetron sputtering IrMn top spinvalve. Thin Solid Films 441:111–114

Martin CR, Baker LA (2005) Expanding the molecular electronics toolbox. Science 309:67–68

Namatsu H, Takahashi Y, Yamazaki K, Yamaguchi T, Nagase M, Kurihara K (1998) Three-dimensional siloxane resist for the formation of nanopatterns with minimum linewidth fluctuations. J Vac Sci Technol B16:69–76

Pramanik S, Stefanita C-G, Bandyopadhyay S (2006) Spin transport in self assembled all-metal nanowire spin valves: a study of the pure Elliott–Yafet mechanism. J Nano Sci Tech 6:1973–1978

Qin L, Park S, Huang L, Mirkin CH (2005) On-wire lithography. Science 309:113–115

Springham SV, Osipowicz T, Sanchez JL, Gan LH, Watt F (1997) Micromachining using deep ion beam lithography. Nucl Instr Meth B130:155–159

Szymanski R, Jamieson DN (1997) Ion source brightness and nuclear microprobe applications. Nucl Instr Meth B130:80–85

Thelander C, Agarwal P, Brongersma S, Eymery J, Feiner LF, Forchel A, Scheffler M, Riess W, Ohlsson BJ, Gösele U, Samuelson L (2006) Nanowire-based one-dimensional electronics. Materialstoday 9:28–35

Udalagama CNB, Bettiol AA, van Kan JA, Teo EJ, Breese MBH, Watt F (2007) The rapid secondary electron imaging system of the proton beam writer at CIBA. Nucl Instr Meth B260:390–395

van Kan JA, Sum TC, Osipowicz T, Watt F (2000) Sub 100 nm proton beam micromachining: theoretical calculations on resolution limits. Nucl Instr Meth B161–163:366–370

van Kan JA, Bettiol AA, Wee BS, Sum TC, Tang SM, Watt F (2001) Proton beam micromachining: a new tool for precision 3D microstructures. Sens Actuators A92:370–374

van Kan JA, Bettiol AA, Watt F (2003a) Three-dimensional nanolithography using proton beam writing. Appl Phys Lett 83:1629–1631

van Kan JA, Bettiol AA, Watt F (2003b) Proton beam nanomachining: end station design and testing. Mat Res Soc Symp Proc 777:T2.1.1

van Kan JA, Bettiol AA, Ansari K, Shao PG, Watt F (2004a) Improvement in proton beam writing at the nano scale. Proc IEEE MEMS 673–676

van Kan JA, Bettiol AA, Ansari K, Teo EJ, Sum TC, Watt F (2004b) Proton beam writing: a progress review. Int J Nanotechnol 1(4):464–479

van Kan JA, Shao PG, Molter P, Saumer M, Bettiol AA, Osipowicz T, Watt F (2005) Fabrication of a free standing resolution standard for focusing MeV ion beams to sub 30 nm dimensions. Nucl Instr Meth B231:170–175

van Kan JA, Bettiol AA, Watt F (2006) Proton beam writing of three-dimensional nanostructures in hydrogen silsesquioxane. Nano Lett 6:579–583

van Kan JA, Bettiol AA, Chiam SY, Saifullah MSM, Subramanian KRV, Welland ME, Watt F (2007) New resists for proton beam writing. Nucl Instr Meth B260:460–463

Waligorski MPR, Hamm RN, Katz R (1986) The radial distribution of dose around the path of a heavy ion in liquid water. Nucl Tracks Radiat Meas 11:309–319

Watt F, van Kan JA, Rajta I, Bettiol AA, Choo TF, Breese MBH, Osipowicz T (2003) The national university of singapore high energy ion nano probe facility performance tests. Nucl Instr Meth B210:14–20

Zhang F, van Kan JA, Chiam SY, Watt F (2007) Fabrication of free standing resolution standards using proton beam writing. Nucl Instr Meth B260:474–478